

FINITENESS OF THE COULOMB GAUGE QCD PERTURBATIVE EFFECTIVE ACTION

A. ANDRAŠI AND J. C. TAYLOR

ABSTRACT. At 2-loop order in the Coulomb gauge, individual Feynman graphs contributing to the effective action have energy divergences. It is proved that these cancel in suitable combinations of graphs. This has previously been shown only for transverse external fields. The calculation results in a generalization of the Christ-Lee term which was inserted into the Hamiltonian.

Date: February 9, 2015.

1991 Mathematics Subject Classification. PACS: 11.15,Bt; 03.70.+k.

Key words and phrases. QCD, Coulomb gauge, effective action.

1. INTRODUCTION

In QCD, the Coulomb gauge has some attractions. It is the only manifestly unitary gauge (no ghosts). It may be convenient in practice when there is a natural rest frame, as in thermal QCD or for heavy quarks. It has been used in studies of confinement (see for example [2]). It has been used in lattice calculation, see for example [1], and in studies of infra-red behaviour (see [3]). But, in perturbation theory, it has complications due to *energy divergences*, that is Feynman integrals which are divergent over the internal energy integrals (for fixed spatial momenta). These divergences appear at 1-loop order, but in this case are easily curable (see [4]), most simply by using, instead of the Lagrangian formalism, the phase-space, Hamiltonian formalism, as we do in this paper.

At 2-loop order, there are more subtle energy divergences. These occur in divergent integrals of the form

$$(1) \quad \int dp_0 dq_0 \frac{p_0}{p_0^2 - P^2 + i\epsilon} \frac{q_0}{q_0^2 - Q^2 + i\epsilon} F(\mathbf{P}, \mathbf{Q}, \mathbf{R})$$

(capital letters, $\mathbf{P}, \mathbf{Q}, \mathbf{R}$ etc denote spatial momenta and $P \equiv |\mathbf{P}|$ etc). This problem is resolved if it can be shown that graphs can be grouped so that integrals like (1) appear in the combination

$$(1/3) \int dp_0 dq_0 dr_0 \delta(p_0 + q_0 + r_0) F(\mathbf{P}, \mathbf{Q}, \mathbf{R})$$

$$\times \left[\frac{p_0}{p_0^2 - P^2 + i\epsilon} \frac{q_0}{q_0^2 - Q^2 + i\epsilon} + \frac{q_0}{q_0^2 - Q^2 + i\epsilon} \frac{r_0}{r_0^2 - R^2 + i\epsilon} + \frac{r_0}{r_0^2 - R^2 + i\epsilon} \frac{p_0}{p_0^2 - P^2 + i\epsilon} \right]$$

$$(2) \quad = -(\pi^2/3) F(\mathbf{P}, \mathbf{Q}, \mathbf{R})$$

as may be shown by contour integration.

For definiteness, suppose that we are calculating, to 2-loop order, the effective action $\Gamma(A_i^a)$ as a functional of the external vector field A_i^a (i, j, \dots are spatial indices and a, b, c, \dots denote colour). (Parts of Γ depending on A_0^a or E_i^a contain no divergent integrals like (1).)

The requisite theorem, that graphs can be combined to give (2), was proved by Doust [6] (see also [7]) for the special case of transverse external fields, $\partial_i A_i^a = 0$. But the effective action is formally defined (see the Appendix) for general A_i^a , and this is indeed required in order to state the BRST identities for Γ . The purpose of the present paper is to extend Doust's theorem to general A_i^a . The $O(g^4)$ case was already studied in [8]. The divergent integrals (1) are connected with the fact that

operator ordering of the Hamiltonian (which is non-polynomial) may not be well-defined. Christ and Lee [5] (and references therein) argued that the correct ordering entailed adding onto the naive Hamiltonian two operator functionals, called V_1 and V_2 , of the operator \hat{A}_i^a , which in the Coulomb gauge is transverse by definition. To avoid double counting, the Feynman integrals (1) and (2) would have to be omitted. Doust found that the integrals (2) contributed the same functionals $V_1 + V_2$ to the effective action.

1.1. The flow gauge. In order to manipulate integrals like (1) rigorously, a temporary regularization is necessary. Dimensional regularization (which we use, with space-time dimension d , to control ordinary ultra-violet divergences) does not have any effect on (1). So we (following Doust) employ a 'flow gauge' with a parameter θ . For finite θ the function F in (1) depends also on $\theta p_0, \theta q_0, \theta r_0$ so as to make the integral converge. So in (1) and (2) we must replace F by (we write p for the Lorentz vector $(p_0; \mathbf{P})$)

$$(3) \quad F(\mathbf{P}, \mathbf{Q}, \mathbf{R}, \theta p_0, \theta q_0, \theta r_0) = F(p, q, r).$$

The Coulomb gauge is the limit $\theta \rightarrow 0$, which we take only after getting the combinations (2). ($\theta = 1$ is the Feynman gauge, so the flow gauge is sometimes called an interpolating gauge). The flow gauge is defined by the gauge-fixing term

$$(4) \quad -\frac{1}{2\theta^2}[(\partial_i \hat{A}_i^a)^2 - \theta^2(\partial_0 \hat{A}_0^a)^2]$$

(the limit $\theta \rightarrow 0$ imposes the transversality condition on the operator \hat{A}_i^a). The effect of this is that the bare Coulomb propagator, $-1/P^2$, is everywhere replaced by

$$(5) \quad -\frac{1}{P^2 - \theta^2 p_0^2} \equiv -\frac{1}{P^2}$$

proof.tex This is what causes the function F in (1) and (2) to be replaced by (3).

In the Coulomb gauge, ghost loops exactly cancel closed Coulomb loops. But in the flow gauge this is not exactly the case. Ghosts, but not Coulomb loops, have a coupling $O(\theta^2)$ to the Coulomb field. Hence, as well as graphs similar to Fig.1, graphs with ghost loops have to be included in the proof. When the convergent form (2) is finally attained, the ghost graphs can be omitted.

The method of our proof, following [6], is to show that $F(p, q, r)$ is a cyclically symmetric function of its arguments. Then the integrand in (1) can be symmetrized, to give (2). Finally, having attained the convergent combination in the square bracket in (2), the limit $\theta \rightarrow 0$ can be taken in F in (2) giving the Coulomb gauge.

1.2. An example. An example (at $O(g^7)$) of a Feynman graph leading to an integral of the form of (1) is shown in Fig.1. Our notation for Feynman graphs is explained in Fig.2. Dotted lines denote the propagator (5). Dashed lines denote the propagator for \hat{A}_i^a (transverse in the Coulomb gauge, but not transverse for nonzero θ). Solid lines always denote a momentum (either spatial or time-like), multiplied by i , in the numerator (the sense of the momentum being directed towards the neighbouring vertex). The external dashed lines represent the external field A_i^a . In Fig.1, the two denominators in (1) come from the lines labeled p' and q in Fig.1.

In the Coulomb gauge ($\theta = 0$) all the relevant graphs have a 'spine' coming from the Coulomb operator in the Hamiltonian. In Fig.1 this spine consists of the

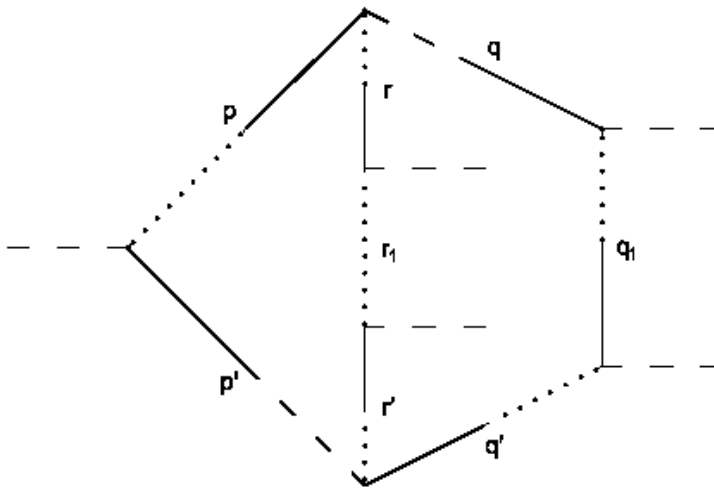


Fig.1 An example of a graph $O(g^7)$ giving an integral of the form (1).

p, r, r_1, r', q', q_1 lines. In addition to this spine, there are two lines (q, p') where \hat{A}_i and \hat{E}_j operators in the Coulomb operator have been contracted with one-another. In the flow gauge, the structure of the graphs are the same though their interpretations are not as simple.

In Fig.1 there is just one line, labeled r_1 , which has a dotted line with no solid line on it. In all the relevant graphs there is on the spine just one line like this, which may be in any position, on the centre line or the righthand or lefthand one. (To order g^n there are $n - 1$ such possible positions). In the case of transverse A_i^a , treated by Doust, the contribution is independent of the position of this line, which simplifies the argument. We show that the proof can be made without this simplifying property.

We need a compact notation in order to write down the general graphs giving integrals of the form of (1). This we explain in the next section.

2. THE GHOST AND COULOMB PROPAGATORS

The example in Fig.1 has three *chains* of lines. Each chain consists partly of a propagator in the external field A_i^a . On the left and right in Fig.1, these propagators have the same form as the ghost propagator (though they are not ghost lines), and in the centre the Coulomb propagator occurs. We need a compact notation for these two propagators, which we now give.

$$\begin{array}{l}
 \begin{array}{c}
 \text{---} i \text{---} j \\
 \dots\dots\dots \\
 \xrightarrow{E_m} \text{---} A_j \\
 \xrightarrow{m} \text{---} n \\
 \xrightarrow{E_m} \text{---} A_0 \\
 \text{---} 0 \text{---} n \\
 \text{====}
 \end{array}
 \begin{array}{l}
 -\frac{1}{k^2 + i\eta} \left[\delta_{ij} - \frac{K_i K_j}{K^2 - \theta^2 k_0^2} \right] \\
 -\frac{1}{K^2 - \theta^2 k_0^2} \\
 -\frac{ik_0}{k^2 + i\eta} \left[\delta_{mj} - \frac{K_m K_j}{K^2 - \theta^2 k_0^2} \right] \\
 -\frac{K^2}{k^2 + i\eta} \left[\delta_{mn} - \frac{K_m K_n}{K^2} \right] \\
 \frac{iK_m}{K^2 - \theta^2 k_0^2} \\
 -\frac{iK_n}{K^2 - \theta^2 k_0^2} \\
 -\frac{1}{K^2 - \theta^2 k_0^2}
 \end{array}
 \end{array}$$

(-1) for each closed ghost loop

$(2\pi)^4 i$ for each vertex

$\frac{1}{(2\pi)^4 i}$ for each propagator

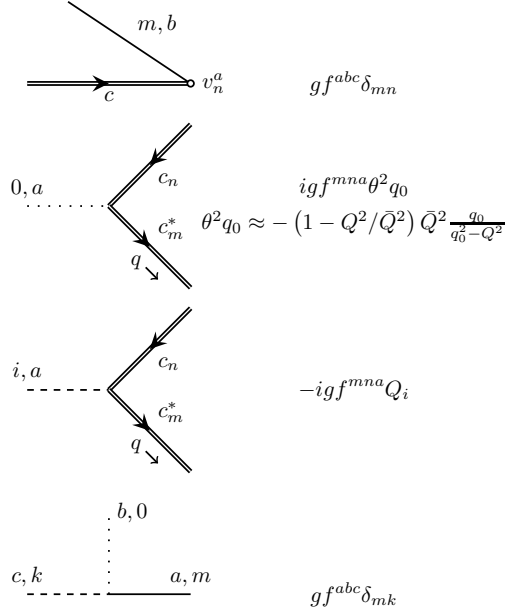


Fig. 2: The graphical notation for Feynman propagators and the rules for vertices in the flow gauge. Doubled lines represent ghosts.

We call the ghost propagator $G^{aa'}(\mathbf{P}, \mathbf{P}'; \theta p_0, \theta p'_0)$. In the Coulomb gauge, there would be no dependence on p_0, p'_0 , but in the flow gauge, such dependence is introduced through the denominators (5).

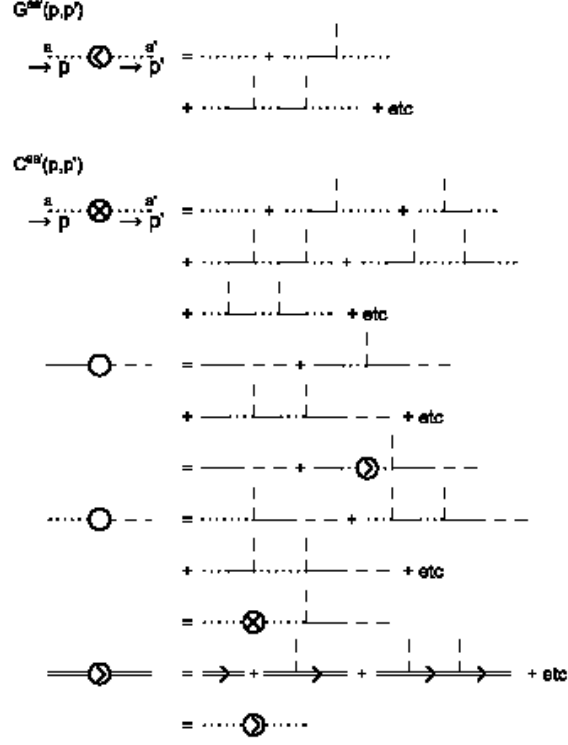


Fig.3 Definitions of graphical symbols and relations between them.
The first two definitions correspond to equations (7) and (9).

Define the antisymmetric matrix field

$$(6) \quad A_i^{ab}(k) = f^{abc} A_i^c(k)$$

where $A_i^c(k) = A_i^c(-k)$ is the external field in momentum space.

The ghost propagator G is defined by the integral equation

$$(7) \quad -\overline{P^2} G^{aa'}(p, p') = \delta^{aa'} \delta^d(p - p') + ig \int d^d p_1 \mathbf{P} \cdot \mathbf{A}^{ab}(p_1 - p) G^{ba'}(p_1, p').$$

This may be solved iteratively to give a series in g . As an example, the second order term is

$$(8) \quad g^2 \int d^d p_1 [\overline{P^2 P_1^2 P'^2}]^{-1} \mathbf{P} \cdot \mathbf{A}^{ab}(p_1 - p) \mathbf{P}_1 \cdot \mathbf{A}^{ba'}(p_1 - p').$$

The Coulomb propagator $C^{aa'}(p, p')$ is given in terms of the ghost propagator by

$$(9) \quad C^{aa'}(p, p') = \int d^d p_1 G^{ab}(p, p_1) (-\mathbf{P}_1^2) G^{a'b}(-p', -p_1).$$

As an example, one of the three second order terms in C is

$$(10) \quad g^2 \int d^d \mathbf{P}_1 [\overline{P^2 P_1^2 P'^2}]^{-1} \mathbf{P} \cdot \mathbf{A}^{ab}(p_1 - p) \mathbf{P}' \cdot \mathbf{A}^{a'b}(p' - p_1).$$

The example (10) occurs on the centre chain in Fig.1 (with p replaced by r). Note the difference between (8) and (10) in general, but for transverse A they are equal.

The series for G and C are illustrated graphically in Fig.3.

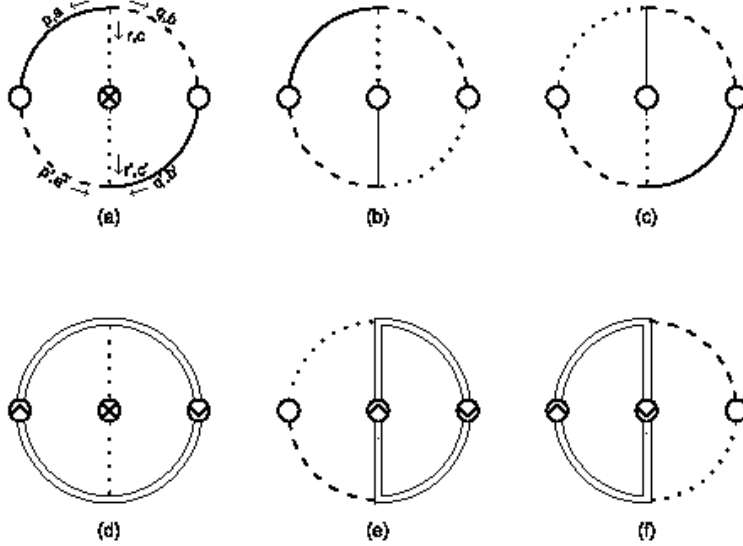


Fig.4 The structure of graphs contributing to the divergent integral (1). Each line represents a chain of arbitrarily many propagators, as defined in Fig.3.

3. THE ENERGY-DIVERGENT GRAPHS

We need a notation for graphs in which an arbitrary number of external gluon fields are attached to the three chains. This notation is shown in Fig.3. Then the six types of graph which give an integral containing (1) (with the substitution (5)) are shown in Fig.4. They are all drawn with the p -chain on the left and the q -chain on the right. These graphs give contributions of the form

$$(11) \quad \frac{1}{2}(2\pi)^{-d} f^{abc} f^{a'b'c'} \int d^d p d^d q d^d r \delta(p + q + r) d^d p' d^d q' d^d r' \delta(p' + q' + r') \left[\frac{p_0}{p^2} \frac{q'_0}{q'^2} \right] B,$$

where the factors B will be expressed graphically in Figs.7 and 8 later in this section. (The factor $1/2$ in (11) is needed because the set of graphs which we use has symmetry under the interchange of the two internal vertices.)

In order to connect (11) to (1), we need a lemma. This states that, up to terms $O(\theta)$, we may replace $(p_0 q'_0)/(p^2 q'^2)$ or $p'_0 q_0/(p'^2 q^2)$ by

$$(12) \quad \frac{p_0}{p^2 + i\epsilon} \times \frac{q_0}{q_0^2 + i\epsilon}$$

(reminding ourselves of the $i\epsilon$ factors, which we usually leave understood). The proof is as follows. The difference is an integral of the form

$$(13) \quad \int dp_0 dq_0 dr_0 \delta(p_0 + q_0 + r_0) \left[\frac{p_0 q'_0}{p^2 q'^2} - \frac{p_0 q_0}{p^2 q^2} \right] F(\mathbf{P}, \mathbf{Q}, \mathbf{R}; \theta p_0, \theta q_0, \theta r_0; \theta k_0^{(m)}, \mathbf{K}^{(m)})$$

where the $k^{(m)}$, ($m = 1, 2, 3..$) are external gluon momenta. Also $q'_0 - q_0$ is equal to a linear combination of a subset of the $k_0^{(m)}$. We now make a change of variables

$$(14) \quad \check{p}_0 = \theta p_0, \check{q}_0 = \theta q_0, \check{r}_0 = \theta r_0.$$

Then, in terms of the new variables of integration, the difference between the two terms in the square bracket in (13) lies in dependence on $\theta^2 P^2, \theta^2 P'^2, \theta k_0^{(m)}$. The integral is convergent, because of the terms in F like

$$(15) \quad \frac{1}{\check{r}_0^2 - \theta^2 \mathbf{R}^2};$$

so we may let $\theta \rightarrow 0$, and the integrand in (13) is zero in the limit.

In view of this lemma, the square bracket in (11) may be replaced by (1). Having done this, the contributions to B in (11) may, with the use of the definitions in Figs.3 and 5, be written as in Fig.7. All these graphs have at least one external field attached to the p -chain and at least one to the q -chain (these are the external dashed lines shown explicitly; in addition there are arbitrarily many attachments in the C and D propagators). But there are the special cases in which there is no external attachment to the p -chain, or none to the q -chain, or none to either. Some examples of these cases are shown in Fig.8. Our aim is to show that the sum of the graphs in Figs.7 and 8 has symmetry under cyclic permutations of

$$(16) \quad (p, p'; a, a'), (q, q'; b, b'), (r, r', c, c').$$

Then, with the integration (11), (1) can be replaced by the convergent integral (2).

To order g^n , there are contributions with either $n + 1$ or n or $n - 1$ denominators like (5). It turns out that each of these three classes separately has cyclic symmetry; so we treat them one by one in the following subsections.

3.1. $(n + 1)$ denominators. For these terms, in the graphs in Fig.7, we take the $P_i P_j / \bar{P}^2$ and P^2 / \bar{P}^2 terms from Fig.5. We then use the first two identities in Fig.6, which follow from (7) and (9), thus getting one contribution from (a) and two each from (b), (c), (d), (e) and (f). In the ghost graphs (d), (e) and (f), we use also the third identity in Fig.6, which follows from momentum conservation. As a result of these steps, there are finally four contributions from each of (d), (e) and (f). The total number of contributions from all six graphs is thus 17. There are sign factors. The ghost graphs (d), (e), (f) each have a minus sign. There are additional minus signs for (a), (d), (e) and (f) because their colour matrices are in a different order from that in equation (11). Finally, contributions from the last term in the second identity in Fig.6 receive another minus sign. The term from (a) is canceled by one of the contributions from (d), so that fifteen graphs remain. These fall into five triplets, each triplet being invariant under cyclic permutations of the

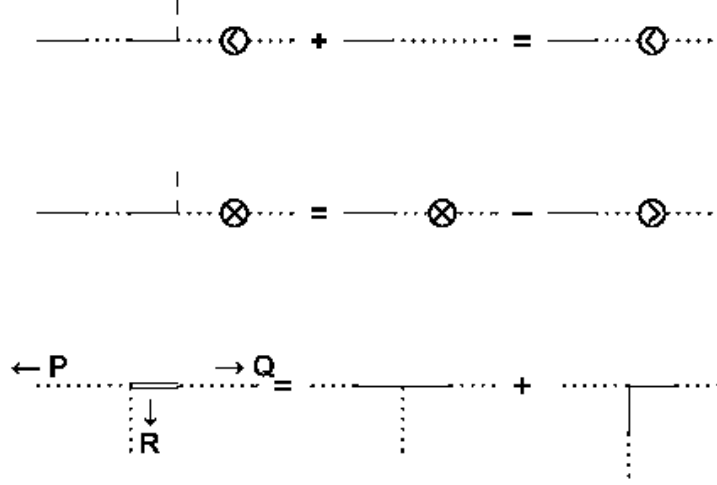


Fig.6 Three identities expressed graphically. The first two follow from the defining equations (7) and (9) or from Fig.3. The third is a consequence of momentum conservation $P + Q + R = 0$.

where $A_I^{cc'}(k)$ is the external field shown explicitly by the dashed lines in Fig.10. Expression (19) is symmetric in p, q, r .

In Fig.10, use has already been made of the first identity in Fig.6. To simplify these graphs, we use the third identity in Fig.6 for graphs (d) and (f), and apply Jacobi identity, shown graphically in Fig.11, to graphs (d), (ei) (eii). This identity, stated algebraically, is

$$(20) \quad f^{abc'} A_i^{cc'} = f^{ab'c} A_i^{b'b} + f^{a'bc} A_i^{a'a},$$

where $A_i^{cc'}$ is defined in (6). There result 14 graphs. Graph (a) cancels one of the contributions from (d), when we make use of (17). Again using (17) where necessary, we obtain 12 graphs, which fall into four groups of three, each group having cyclic symmetry. These are shown in Fig.12, labeled with the names of the graphs in Fig.10 from which they originate. Again, the cyclic symmetry enables us to replace the divergent (1) by the convergent (2).

3.3. $(n - 1)$ denominators. In this case, we take two terms δ_{ij} or 1 from Fig.5 in Fig.7. The results are shown in Fig.13. Then we use the Jacobi identity Fig.11 twice in graph (d) and once each in graphs (e) and (f). There result 11 graphs. Graph (a) cancels one of the contributions from (d), leaving nine graphs. These fall into three cyclically symmetric triplets, as shown in Fig.14, having used the inversion

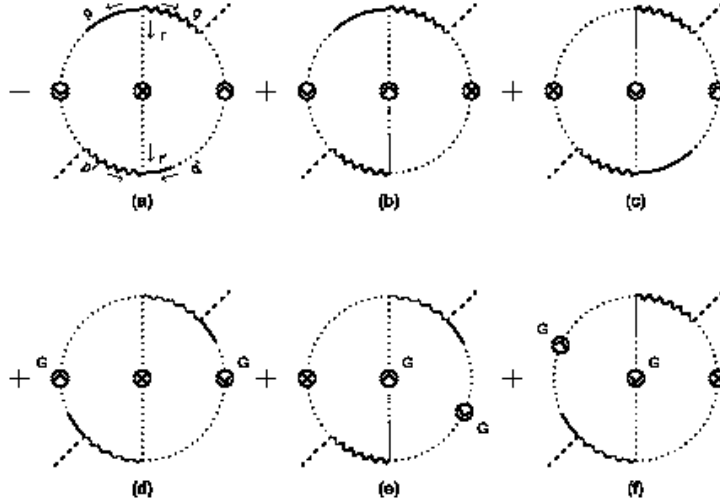


Fig.7 Graphs derived from Fig.4. which contribute to the factor B in equation (11). The notation is defined in Figs. 3 and 5.

symmetry in (18) where necessary. Once again, the cyclic symmetry enables the divergent (1) to be replaced by the convergent (2) in (11).

This completes the proof for graphs in which at least one external field A is attached to each chain. But there are exceptional graphs for which this is not the case, like those in Fig.8. We must now deal with these exceptional cases.

4. EXCEPTIONAL GRAPHS

These are graphs with either no external gluon attached to the q -chain or none attached to the p -chain. Because of reflection symmetry (17), we can without loss of generality take the former case. The graphs are shown in Fig.8. Again we have to consider the cases with $(n + 1)$, n , or $(n - 1)$ denominators, but the first of these is already included in the previous section, so we need only consider the latter two cases.

4.1. n denominators. The relevant graphs are shown in Fig.15, where the central rectangle denotes $\delta^{bb'}$ in the graphs (d), (e), (f); and $\delta^{bb'}\delta_{ij}$ in (a), (b), (c). The graphs (ci) , (cii) , (ei) , (eii) arise because of the use of the second identity in Fig.6. The last identity in Fig.6 (momentum conservation) is applied to graph (d) in Fig.15 to give the three graphs in Fig.16.

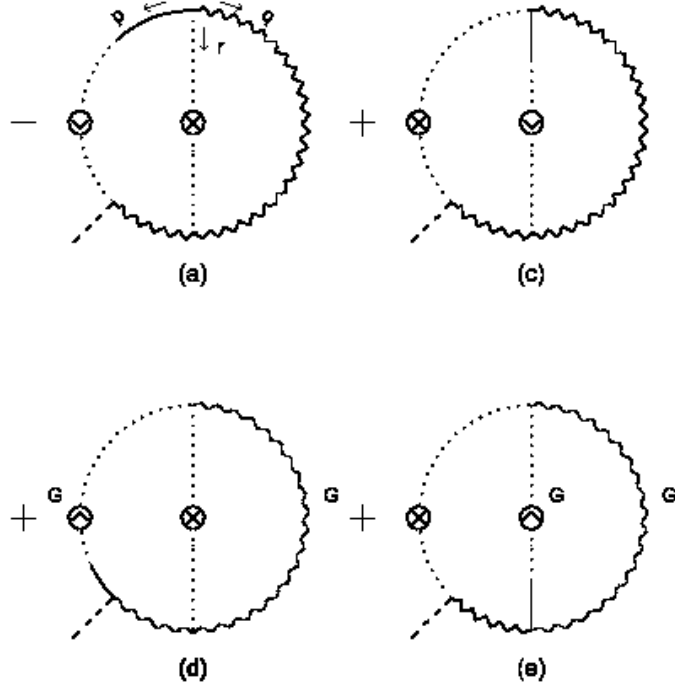


Fig.8 Graphs derived from Fig.4, which contribute to the factor B in equation (11), and which have no external field attached to the q -line. The labels correspond to those in Fig. 7.

We then prove symmetry under the interchange of the p - and r -chains. Graph (a) in Fig.15 cancels graph (dii) in Fig.16. Graphs (cii) and (eii) in Fig.16 each separately have the required symmetry, making use of inversion invariance under (18). And the two pairs

$$(21) \quad \{(ci)', (d\gamma)\}; \{(ei), (d\alpha)\}$$

each are invariant under the interchange.

This means that in (1),

$$(22) \quad F(p, q, r) = F(r, q, p)$$

($F(\mathbf{P}, \mathbf{Q}, \mathbf{R})$ becomes $F(p, q, r)$ in the flow gauge, as in (3)). Therefore we can replace (1) by

$$(23) \quad (1/2) \int dp_0 dq_0 dr_0 \delta(p_0 + q_0 + r_0) F(p, q, r) \left[\frac{p_0}{p_0^2 - P^2 + i\epsilon} \frac{q_0}{q_0^2 - Q^2 + i\epsilon} + \frac{q_0}{q_0^2 - Q^2 + i\epsilon} \frac{r_0}{r_0^2 - R^2 + i\epsilon} \right].$$

We note also that, in Figs.(15) and (16), F factorizes

$$(24) \quad F = \phi_i^{aa'}(\mathbf{P}, \theta^2 p_0^2) \phi_i^{cc'}(\mathbf{R}, \theta^2 r_0^2),$$

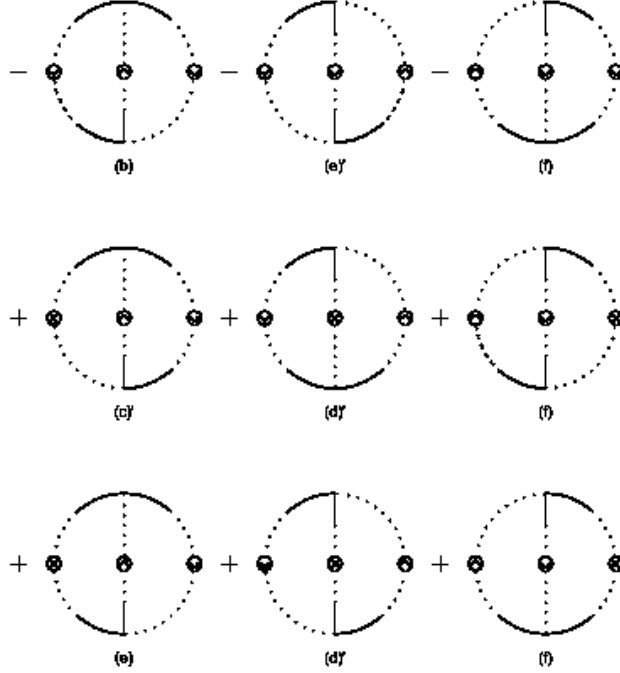


Fig.9 Three triplets of graphs obtained from Fig. 7 by use of the identities in Figs. 3 and 6. Each triplet is invariant under cyclic permutations of its three chains. In addition there are two more triplets obtained from the first and second triplets above by the transformation (17) (reflection). The letters under the graphs indicate the graphs in Fig.7 from which they are derived. The prime on (e)' etc. indicates that the transformation (18) (inversion) has been made. The signs attached to these graphs come about as explained in the text.

neglecting terms $O(\theta k_0^{(m)})$ where $k^{(m)}$ are external momenta; so

$$(25) \quad \int dp_0 \frac{p_0}{p^2} \phi_i^{aa'} = O(\theta),$$

and similarly for the r -integral (just as at one loop order). This allows us to insert the third term $(p_0 r_0 / p^2 r^2)$ into the square bracket in (23) and then use the identity in (2) to get

$$(26) \quad -(\pi^2/2)F$$

and finally let $\theta \rightarrow 0$. Thus we have achieved our aim, but there is the important difference from section 3 that we here have a factor of a half rather than a third as in (2).

4.2. $(n - 1)$ denominators. The relevant graphs are in Fig.17. For graph (d), we use the Jacobi identity (Fig.11) twice to get the three graphs in Fig.18. As usual, graph (a) is canceled by (d1)'. The remaining four graphs fall into two pairs

$$(27) \quad \{(e), (d3)\}; \{(c)', (d2)\}$$

each of which has symmetry under the interchange of the p - and r -lines. After that the argument continues exactly as in subsection 4.1.

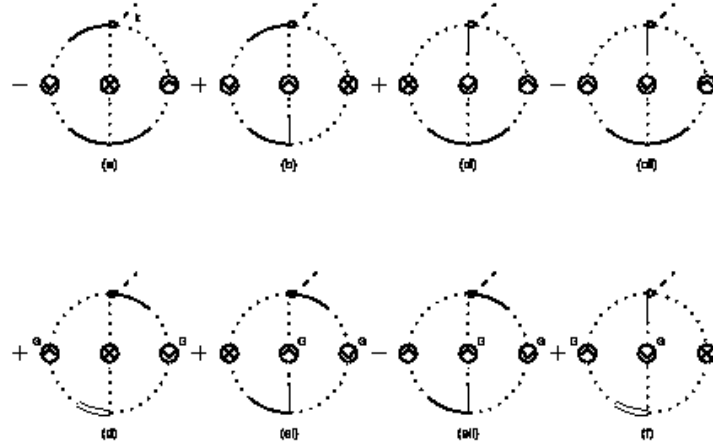


Fig.10 Graphs obtained from Fig.7 with n denominators. The notation is explained in Fig.5. The second identity in Fig.6 has been used, giving (ci), (cii) and (ei), (eii). In each graph, one external field (momentum k) is shown explicitly. To order g^n , the remaining $n-3$ are implicit in the propagators defined in Fig.3.

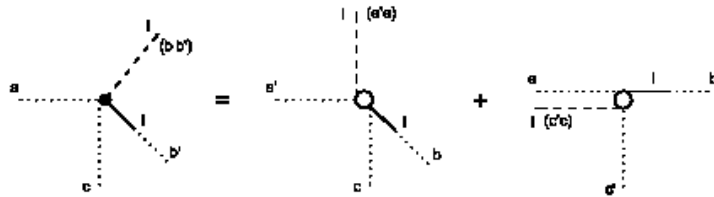


Fig.11 The graphical Jacobi identity expressing equation (20) in the text.

There is a special case in which, in Fig.4, both the p -chain and the q -chain in graph (a) consist of the single terms δ_{ij} , and in graph (d) of the single factors 1. The result is just the same as in [6], and is

$$(28) \quad \pi^2(d-2) \int d^{d-1} \mathbf{P} d^{d-1} \mathbf{Q} d^{d-1} \mathbf{R} \delta^{d-1}(\mathbf{P} + \mathbf{Q} + \mathbf{R}) f^{abc} f^{abc'} C^{cc'}(\mathbf{R}, \mathbf{R}').$$

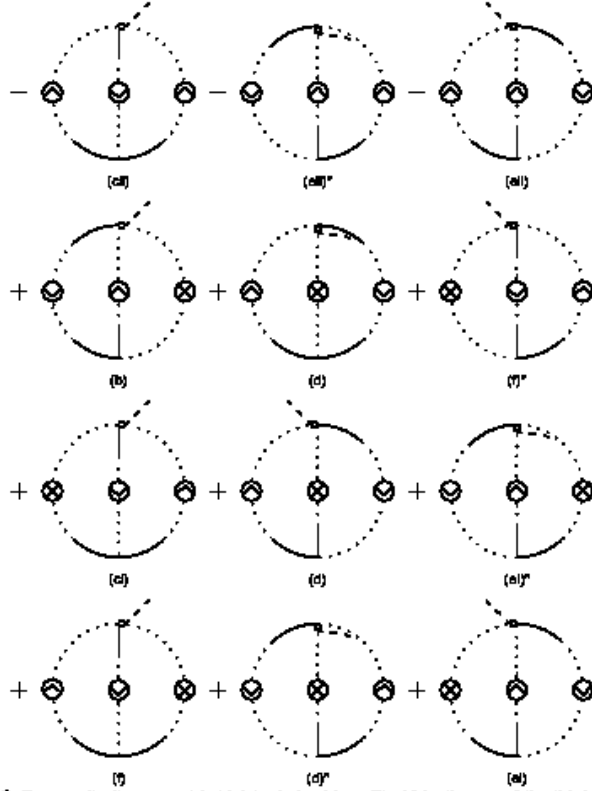


Fig.12 Four cyclically symmetric triplets derived from Fig.10 by the use of the third Identity in Fig.6 and the Jacobi identity in Fig.11. The letters denote the graphs in Fig.10 from which they are derived. The double prime denotes the transform by (17) (reflection).

In dimensional regularization this integral is zero, but we write it here for completeness. Below we neglect all such terms which vanish in dimensional regularization.

5. THE GENERALIZED CHRIST-LEE FUNCTIONS

In both section 3 and section 4, the energy integral has been shown to be finite, and could be done using equation (2). But in section 3 this resulted in a factor $-\pi^2/3$ while in section 4 the factor was $-\pi^2/2$ (leaving aside (28)). The limit $\theta \rightarrow 0$ could be taken. We present the results as the sum of two contributions. For the first we will add together the contributions from sections 3 and 4 with a factor $-\pi^2/3$ for both. In the second contribution, we compensate by using the result of section 4 but with a factor $-\pi^2/6$.

5.1. Contributions from Figs.7, 8. We take the former contribution first, combining all the terms arising from the graphs in Figs.7 and 8. Since we have complete contributions (not separating Fig.8 from Fig.7) the ghost graphs disappear in the limit $\theta \rightarrow 0$, because of the factors $[1 - (P^2/\bar{P}^2)]$ in Fig.5. Thus the result comes from graphs (a), (b), (c) in Fig.7 and (a), (c) in Fig.8. It is straightforward to write these out using the rules in Figs.3 and 5.

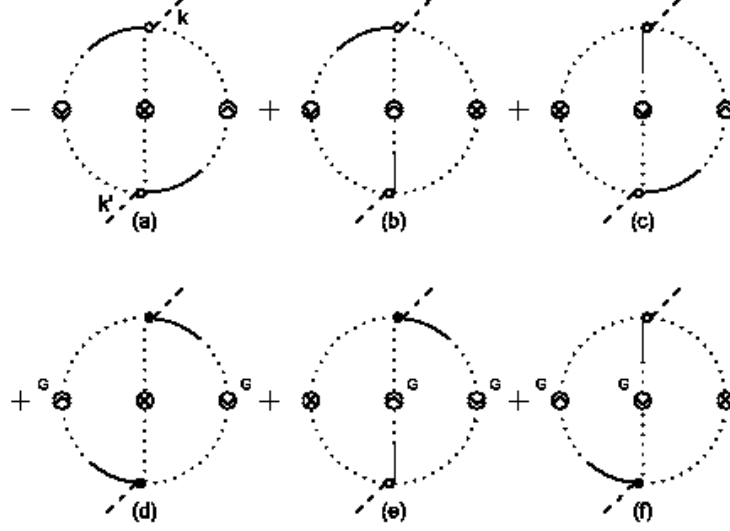


Fig.13 Graphs with $n-1$ denominators contributing to the factor B in equation (11). They are derived from Fig.7 using Fig.5.

We first note that, with $\theta = 0$, the only external momentum dependence in (11) comes from the second δ function:, which we may write

$$(29) \quad \delta(p'_0 + q'_0 + r'_0) = \delta \left[\sum_m k_0^{(m)} \right] = \frac{1}{2\pi} \int dt \exp \left(-it \sum_m k_0^{(m)} \right)$$

where the $k^{(m)}$ ($m = 1, 2, 3, \dots$) are the momenta in the external fields. The effect of this is that the external field $A_i^a(\mathbf{K}, k_0)$ is everywhere replaced by the time Fourier transform $\tilde{A}_i^a(\mathbf{K}, t)$. From now on, that external fields in (7), (9) and (31), (32), (33) below are to be understood as meaning this.

Then the contributions have the form

$$(30) \quad -(g^2/8)(2\pi)^{-d+1} f^{abc} f^{a'b'c'} \int dt \int d\mathbf{P} d\mathbf{Q} d\mathbf{R} d\mathbf{P}' d\mathbf{Q}' d\mathbf{R}' \delta(\mathbf{P} + \mathbf{Q} + \mathbf{R}) \delta(\mathbf{P}' + \mathbf{Q}' + \mathbf{R}') F,$$

where the terms in F come from the graphs mentioned above. (In (30), the integrals and delta functions are understood to be $(d-1)$ -dimensional.) Expression (30) is for the effective action; for an effective Hamiltonian, the time integral and the minus sign should be omitted.

Define

$$J_{ii'}^{aa'}(\mathbf{P}, \mathbf{P}') = T_{ii'}(\mathbf{P}) \delta^{aa'} \delta(\mathbf{P} - \mathbf{P}')$$

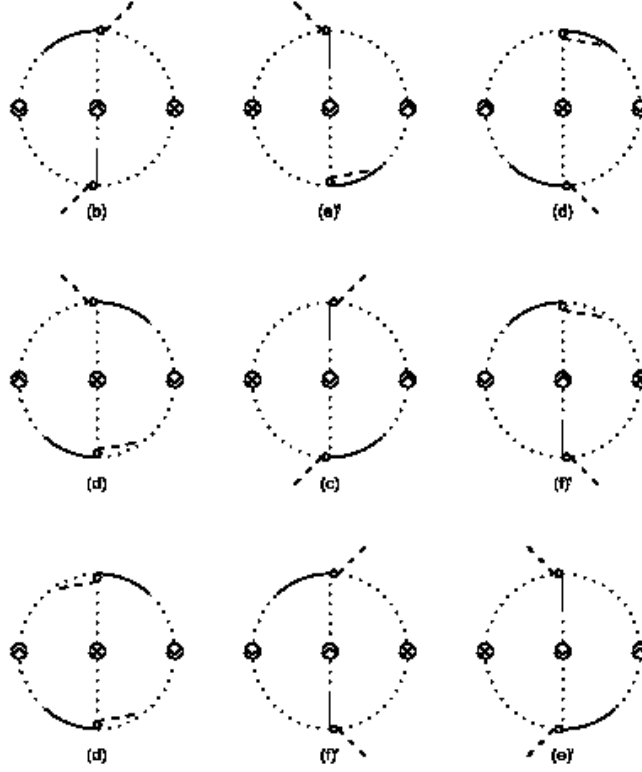


Fig.14 Three cyclically symmetric triplets of graphs derived from Fig.13 by using the Jacobi Identity in Fig.11. The letters denote the graphs in Fig.13 from which they are derived, and a prime denotes inversion under (18).

$$(31) \quad + \int d\mathbf{P}'' T_{i''i}(\mathbf{P}) A_i^{a''}(\mathbf{P} - \mathbf{P}'') G^{a''a'}(\mathbf{P}'', \mathbf{P}') (iP'_{i''})$$

and

$$(32) \quad L_i^{a'a'}(\mathbf{P}, \mathbf{P}') = \int d\mathbf{P}'' T_{i''i}(\mathbf{P}) A_{i''}^{a''a}(\mathbf{P} - \mathbf{P}'') C^{a''a'}(\mathbf{P}'', \mathbf{P}')$$

where the transverse projection operator $T_{i''i}(\mathbf{P}) = \delta_{i''i} - (P_i P_{i''})/P^2$ comes from Fig.5 when $\theta = 0$. With this notation Fig.7(a),(b),(c) together with Fig.8(a),(c) give a contribution to F in (30)

$$(33) \quad \begin{aligned} & (1/3)[-J_{i''i}^{a'a}(-\mathbf{P}', -\mathbf{P}) C^{cc'}(\mathbf{R}, \mathbf{R}') J_{ii''}^{bb'}(\mathbf{Q}, \mathbf{Q}') \\ & + J_{ij}^{a'a}(-\mathbf{P}', -\mathbf{P}) G^{cc'}(\mathbf{R}, \mathbf{R}') L_j^{bb'}(\mathbf{Q}, \mathbf{Q}') (-iR'_i) \\ & + (iR_j) L_i^{a'a}(-\mathbf{P}', -\mathbf{P}) G^{c'c}(-\mathbf{R}', -\mathbf{R}) J_{ji}^{bb'}(\mathbf{Q}, \mathbf{Q}')]. \end{aligned}$$

5.2. Contributions from Figs.15, 17. In this case, unlike the previous one, even when $\theta = 0$, we cannot neglect ghost graphs, because only incomplete ghost graphs appear in Fig.17 (the 1 parts from Fig.5 without the $-P^2/\bar{P}^2$ parts); so we must take all the graphs. As explained above, they are taken with a coefficient 1/6.

Thus the contributions have the form

$$(34) \quad (1/6)[(ci)+(d\gamma)'+(ei)+(d\alpha)+(cii)+(eii)]$$

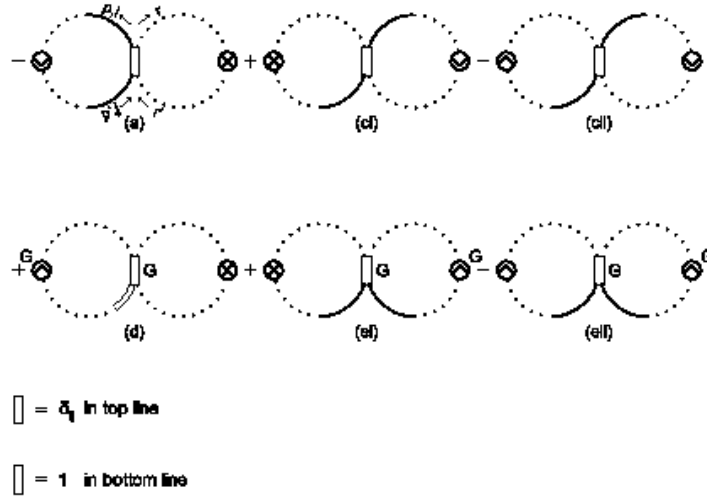


Fig.15 Graphs with n denominators obtained from Fig.8. The q -line (drawn in the center as a thin rectangle) has δ_q in (a) and (c), and 1 in (d) and (e). The second identity in Fig.6 has been used (hence two contributions from (c) and (e)).

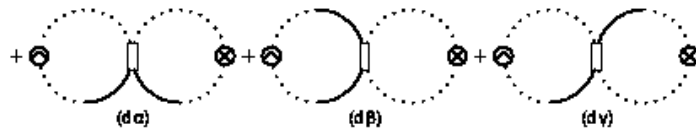


Fig.16 Three graphs obtained from Fig.15 (d) by momentum conservation.

giving

$$(35) \quad (1/3)[(ci)+(ei)+(cii)+(eii)]-(1/6)[(cii)+(eii)].$$

For the first square bracket in (35), we use the identities in Figs.5,6 to get back to graphs like (c) and (e) in Fig.8, but with the q -line replaced by δ_{ij} and 1 respectively. These are shown in Fig.19, and have a coefficient (1/3). This must be doubled because of graphs with the p - and q -lines interchanged. The result is (with the

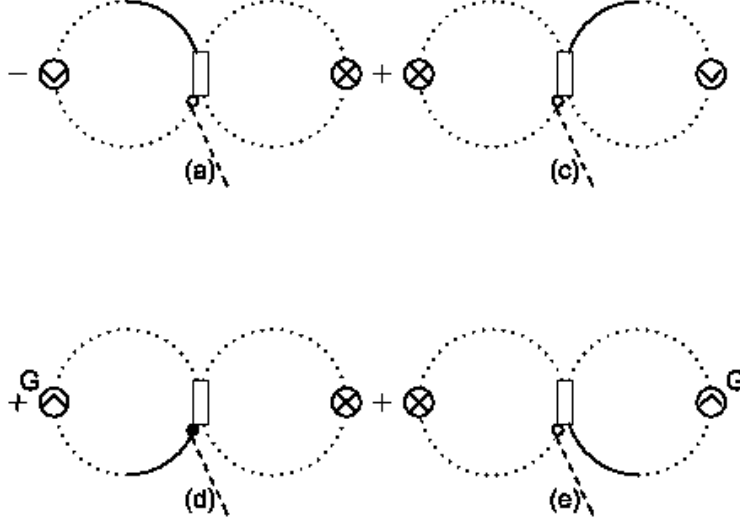


Fig.17 Graphs with $n-1$ denominators obtained from Fig.8. The q-line (drawn in the center as a thin rectangle) has just a $\bar{\delta}_1$ or (in (d)) a 1. The notation of Fig.5 is used.

notation of (32))

$$(36) \quad (1/3)[2L_i^{a'a}(-\mathbf{P}', -\mathbf{P})][\delta^{bb'}\delta(\mathbf{Q}-\mathbf{Q}')][iR_i G^{c'c}(-\mathbf{R}', -\mathbf{R}) - iR'_i G^{cc'}(\mathbf{R}, \mathbf{R}')].$$

There is also the contribution from the second square bracket in (35), with coefficient $(-1/6)$, but there is also a minus sign with (cii) and (eii) in Fig.15. This also must be doubled, giving

$$(37) \quad (1/3)[iP_i G^{aa'}(-\mathbf{P}', -\mathbf{P})][\delta^{bb'}\delta(\mathbf{Q}-\mathbf{Q}')][iR_i G^{c'c}(-\mathbf{R}', -\mathbf{R}) - iR'_i G^{cc'}(\mathbf{R}, \mathbf{R}')].$$

The expressions in (33), (36) and (37), inserted for F in (30), constitute the generalization of the Christ-Lee terms when the external field is not transverse.

6. THE TRANSVERSE SPECIAL CASE

In order to make contact with [5], [6], we show how our result can be re-written if the external gluon field is transverse. In this case, many simplifications occur. The covariant derivative D obeys $\partial \cdot D = D \cdot \partial$ and so

$$(38) \quad G^{aa'}(\mathbf{P}, \mathbf{P}') = G^{a'a}(-\mathbf{P}', -\mathbf{P}),$$

that is the arrows in Figs.3 and 6 and subsequent figures are not necessary.

We examine the contributions to F in equation (30) in this special case. We note that in Fig.17(d), instead of using the Jacobi identity as we did to get Fig.18, we

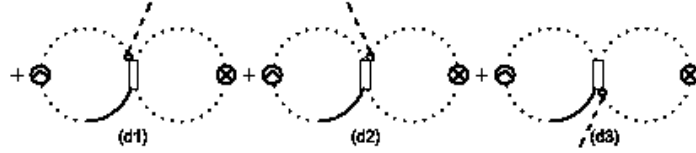


Fig.18 Graphs obtained from Fig.17 (d) by double use of Jacobi Identity.

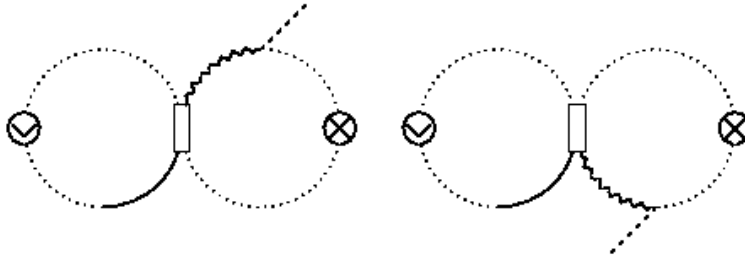


Fig.19 Graphs contributing to the function F in equation (30), which are derived from Figs.15, 16 and 17. They have coefficients $1/3$. The remaining contributions from Fig.15 are the two graphs (ci) and (ei), which have coefficient $-1/6$.

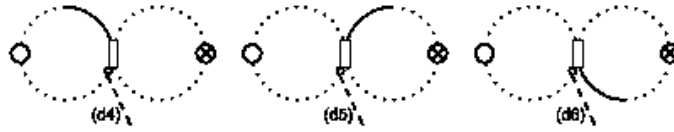


Fig.20 Graphs obtained from Fig.17 (d) by using momentum conservation. These are relevant to the transverse special case, so the arrows are omitted from the left hand lines.

might alternatively use momentum conservation, which yields Fig.20. We will take the average of these two; that is Fig.18 with coefficient $1/6$ together with Fig.20 with coefficient $1/6$. Each of these contributions has to be doubled because of the graphs with p, q interchanged.

Then we take

$$(1/3)[\text{Fig.18} + \text{Fig.15}\{(ci)+(ei)\}] + (1/3)[\text{Fig.20} + \text{Fig.15}\{(ci)+(ei)+(cii)+(eii)\}]$$

$$(39) \quad = (1/3)\text{Fig.19} + (1/3)\text{Fig.21},$$

where we have used the first and second identities in Fig.6. (We neglect terms like (28) which are zero in dimensional regularization.)

In [6], equation (4.5.13), it is shown that the contributions from Fig.7(a),(b),(c) and Fig.8(a),(c) together with (39) are equal to $V_1 + V_2$ of [5]. Thus we have confirmed that, in the transverse special case, our method agrees with the known results.

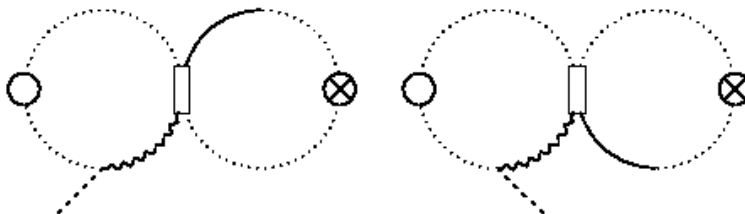


Fig.21 Graphs contributing to the function F in equation (30) derived from Figs.15, 16, 17 and 20. These are relevant to the transverse case, so the arrows are omitted on the left.

7. SUMMARY AND DISCUSSION

We have proved that, in spite of energy divergences in individual 2-loop graphs, the effective action in perturbative Coulomb gauge QCD is well defined. The sum of the relevant terms (in expressions (33), (36) and (37)), which is energy-independent, is calculated, being a generalization of the function $V_1 + V_2$ derived in a different way in [5]. These terms in the effective action would be a necessary contribution to the BRST identities. As a check, we have shown that in the special case of transverse external fields, our result reduces to the known one.

What are the implications of the Christ-Lee function $V_1 + V_2$ and its generalization in this paper? There are two quite different approaches, the Christ-Lee approach [5] and the Doust approach [6]. The Former carefully studies the operator ordering in the Coulomb Hamiltonian, and derives the Hamiltonian

$$(40) \quad H_W + V_1 + V_2$$

where the suffix W denotes Weyl ordering, which is necessary to avoid double counting. This is because of the zero vacuum expectation value of

$$(41) \quad \{\hat{A}_i^a(\mathbf{P})\hat{E}_j^b(\mathbf{P})\}_W \equiv (1/2)\{\hat{A}_i^a(\mathbf{P})\hat{E}_j^b(\mathbf{P}) + \hat{E}_j^b(\mathbf{P})\hat{A}_i^a(\mathbf{P})\},$$

which implies that Feynman graphs like Fig.1, with pairs of operators contracted in the Coulomb potential operator, are omitted.

The Doust approach, followed in this paper, effectively defines the Coulomb gauge as the limit of the flow gauge given by equation (4), and there is no operator ordering problem in the flow gauge.

Presumably the Christ-Lee Hamiltonian (40) might be used in Hamiltonian lattice QCD, but the Doust approach would not be appropriate. On the other hand,

the effective action for non-transverse fields cannot be derived in the Christ-Lee approach; and this general effective action is required to implement BRST identities.

APPENDIX - DEFINITION OF EFFECTIVE ACTION

The effective action is normally defined by first introducing a source current J :

$$(42) \quad \int d^d x J_i^a(x) \hat{A}_i^a(x)$$

(for simplicity, we omit sources for other fields). Then the external classical field $A_i^a(x)$ is introduced by a Legendre transformation from J to A . If the transversality constraint is imposed by a delta function:

$$(43) \quad \delta\{\hat{A}_i^a\}$$

there appears to be a problem, because then only transverse J_i^a contribute in (42).

To avoid this, we may impose transversality by using a gauge-fixing term like

$$(44) \quad \frac{1}{2\theta^2} \int d^d x \{\partial_i \hat{A}_i^a(x)\}^2$$

and taking the limit $\theta \rightarrow 0$ only after the effective action has been defined. Actually, for the purpose of the present paper, we should use the gauge fixing term in equation (4) in place of (44).

REFERENCES

- [1] A. Cucchieri and D. Zwanziger, Nucl. Phys. Proc. Suppl. **53**, 815 (1997); T. Iritani and H. Suganuma, Phys. Rev. D **86**, 074034 (2012); G. Burgio, M. Sschröck, H. Reinhardt, and M. Quandt, Phys. Rev. D **84**, 087704 (2011); A. P. Szczepaniak, E. S. Swanson, Phys. Rev. D **65**, 025012 (2007); S. Szpigiel, G. Krein, R. S. Marques de Carvalho, Braz. J. Phys. **34**, n.1a (2004).
- [2] D. Zwanziger, Nucl. Phys. B **485**, 185 (1997); A. Cucchieri and D. Zwanziger, Phys. Rev. D **65**, 014002 (2002)
- [3] M. le Bellac, P. Reynaud, Nucl. Phys. B **416**, 801 (1994)
- [4] R.N. Mohapatra, Phys. Rev. D **4**, 378, 1007 (1971)
- [5] N. Christ, T. D. Lee, Phys. Rev D **22**, 939 (1980)
- [6] P. Doust, Ann. of Phys. **177**, 169 (1987)
- [7] H. Cheng and E. C. Tsai, Phys.Lett B **176**, 130 (1986)
- [8] A. Andrasi, J. C. Taylor, Ann. of Physics, **407**, 407 (2014)

Current address, Andrasi: Vlačka 58, Zagreb, Croatia

E-mail address, Andrasi: aandrasi@irb.hr

Current address, Taylor: DAMTP, University of Cambridge, Cambridge, UK

E-mail address, Taylor: jct@damtp.cam.ac.uk